Braunschweigische
Wissenschaftliche Gesellschaft

Jahrbuch 2016

Sonderdruck
Seiten 201–216

J. Cramer Verlag · Braunschweig
2017

Magnetic nanoparticles as markers for biomedical analysis*

Meinhard Schilling

Institut für Elektrische Messtechnik und Grundlagen der Elektrotechnik, TU Braunschweig, Hans-Sommer-Straße 66, D-38106 Braunschweig, E-Mail: m.schilling@tu-bs.de

I. Abstract

Magnetic nanoparticles are tiny magnets of the size of large molecules. These nanoparticles can be used as markers for biomedical analysis with remarkable properties. By homogenous magnetic fields they can be rotated and by gradient fields they can be steered with magnetic forces. By antibody functionalization of their surface other proteins can be coupled to the nanoparticles. This way the mobility of the nanoparticle is changed, which can be detected macroscopically by the modified response to external magnetic fields. Protein interaction can help to deliver drugs and to localize infections or inflammations for diagnostic or therapeutic purposes by magnetic particle imaging (MPI).

II. Introduction

The human immune system is almost perfect. By far the most infections are handled without us even noticing it. On our body surface live more bacteria than we have cells in the body. Our bacteria on the inner and outer surfaces of our body amount to more than 1 kg. But within the blood of a healthy human one can find not a single bacterium, since our immune system is our best protection. So we need drugs to support the immune system and in future these drugs should find their targets by themselves.

Magnetic nanoparticles are quite perfect carriers for this purpose in the bloodstream. Their size of 10–30 nm can be as small as a larger protein molecule (hemoglobin 6 nm) and so they can pass all capillary vessels. They can transport drugs everywhere in the body. By functionalization with appropriate antibody molecules they even find their targets themselves, be it bacterial or viral surface

* Der Vortrag wurde am 12.02.2016 in der Klasse für Ingenieurwissenschaften der Braunschweigischen Wissenschaftlichen Gesellschaft gehalten.

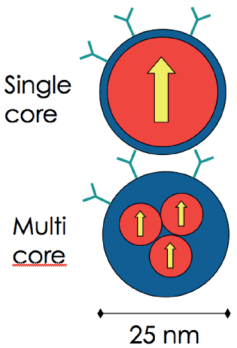

Fig. 1 Nanoparticles

proteins. Additionally, they can even be steered by a magnetic gradient field towards a tumor site. After several passages of the liver, iron-oxide magnetic nanoparticles are metabolized in the human body without problems if their concentration is low enough.

For successful and reliable operation the magnetic nanoparticles have to be throughout characterized, regarding composition, size, form, stabilization, magnetic and chemical properties. During storage these properties should not change. These requirements today are only partly fulfilled. In the chemical preparation process of magnetic nanoparticles it still is almost impossible to produce exactly the same nanoparticles in every batch. During storage, agglomeration and sedimentation can occur and the stabilizing shell for good dispersion and for functionalization can be degrading gradually. Thus, characterization has to control quality and properties again at bedside before application. Here, the methods for a comprehensive quality control of magnetic nanoparticles are reviewed and biomedical applications for magnetic nanoparticles are presented.

III. Properties of magnetic nanoparticles

The toxicity of magnetic nanoparticles depends strongly on their core material. Iron-oxide nanoparticles are regarded mainly as non-toxic, but discussions on differences regarding their iron oxidation state still continue. Nanoparticles can be produced as single core or as multicore particles as depicted in Fig.1.

The first analysis has to ensure that the material composition of the magnetic nanoparticles for biomedical applications excludes cobalt or nickel traces, which should not be applied to mammals, since these metals cannot be metabolized. The second and third step are the determination of the size distribution and the

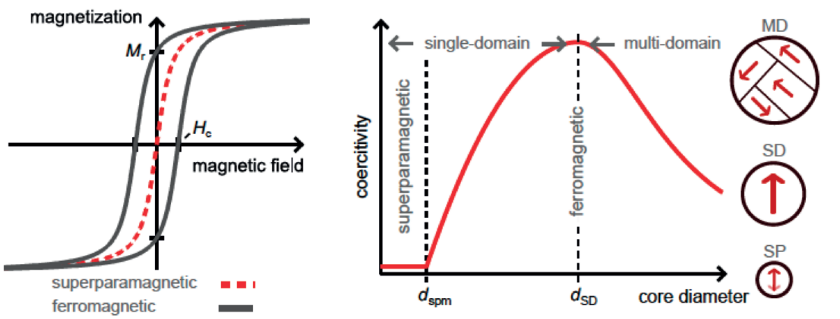

Fig. 2 (a) Dependence of the magnetization on the external magnetic field, (b) dependence of the coercivity on the nanoparticle core diameter.

concentration of magnetic nanoparticles, which are closely related. To get independent measures one often determines the size distribution, but the concentration is analyzed as equivalent iron atoms per volume of water solvent without taking the size distribution into account. The determination of the size distribution is often complicated by agglomeration and cluster formation. In reality, the dispersed nanoparticles can consist of a broad size distribution. So the characterization has to distinguish the thermal distribution governed by the Langevin equation for the thermal activation of the magnetic moment, the core size distribution, the shell thickness distribution, and the distribution of the shell functionalization. Thus a traceable characterization of size distribution, concentration, and particle properties with measurement uncertainties still is an important metrology task for the next years.

The magnetic properties of magnetic nanoparticles strongly depend on the size, as depicted in Fig. 2. In general, magnetic material exhibits magnetization characteristics as depicted in Fig. 2(a). The hysteresis loop is characterized by a coercive field H_c, which depends on the material (hard/soft magnet) by its domain wall pinning properties. The saturation magnetization M_s is reached for high external magnetic fields. In the case of hard magnets the material stays magnetized with the remanent magnetization M_r, even if the external magnetic field is reduced to zero. Large magnetic microparticles are found in a multidomain (MD) state. If the size of the magnet shrinks, the coercive field H_c shows a maximum, if only one domain wall can exist in the particle. For even smaller size the single domain (SD) nanoparticles loose their coercivity and ferromagnetic behavior and enter the region of superparamagnetism (SP). Here, a macroscopic magnetic moment is only established in external magnetic fields and no coercivity is found anymore. The still existing magnetic moment of a single nanoparticle is not aligned by crystalline or surface anisotropy in the material anymore.

The magnetic moment m of a nanoparticle is proportional to the saturation magnetization M_s and its core volume V_c.

$$m = M_s V_C$$

The saturation magnetization M_s depends on the material of the core. If the material properties are well known, the volume distribution is traceable to the distribution of the magnetic moments m. Thus, it is possible, to measure the size distribution magnetically.

In the following only superparamagnetic particles are considered, since they are small enough for biomedical applications in the human body. To measure the magnetic moment distribution the thermal influence expressed by the Langevin function has to be taken into account. Many superparamagnetic moments are not aligned in moderate external magnetic field due to their Brownian motion in the liquid environment of a solvent, most often water. But even immobilized superparamagnetic nanoparticles are not aligned in the moderate magnetic field, but can orient in other directions by the internal degree of freedom, the Néel relaxation. Only rather high external magnetic fields can orient all moments of superparamagnetic nanoparticles into the saturated state. The total energy of the magnetic moment m of an superparamagnetic nanoparticle can be described by [1]

$$E_{ges} = \underset{\text{Internal anisotropy}}{KV \sin^2 \Theta} - \underset{\text{External field}}{mB\cos(\Theta - \Phi)}$$

The first term describes the internal anisotropy energy by its anisotropy constant K, the core volume V_c taking into account the angle Θ between its anisotropy axis and the direction of the external magnetic field. The second term describes the energy of the magnetic moment m in the external flux density B taking into account additionally the angle Φ of the magnetization with respect to the anisotropy axis. For both relaxation mechanisms, Brownian and Nèel relaxation, the energy landscapes are depicted in Fig. 3 with and without external magnetic flux density B. For the description of dispersed nanoparticles all energy contributions of all thermally distributed nanoparticles by the Langevin function have to be integrated over both angles Θ and Φ .

IV. Methods for the characterization of magnetic nanoparticles

Many methods can be applied to characterize magnetic nanoparticles. Due to their small size optical microscopy cannot contribute. Instead scanning electron microscopy SEM and transmission electron microscopy TEM are employed together with scanning probe microscopy AFM and MFM. The crystalline properties are analyzed by x-ray diffraction XRD. The hydrodynamic size distribution

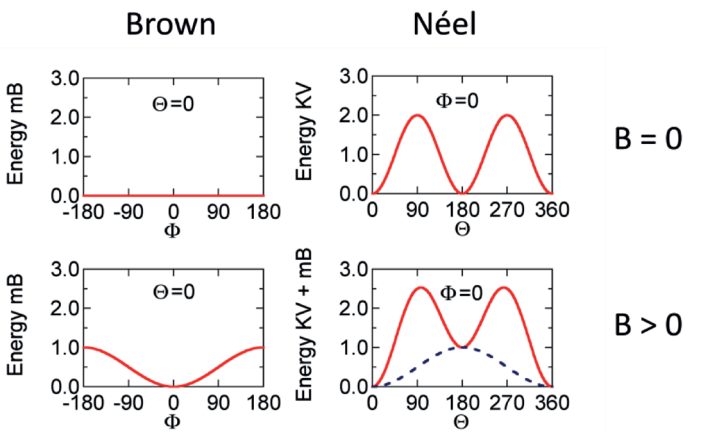

Fig. 3. Dependence of the energy distributions in Brownian and Néel relaxation with and without external magnetic field.

can be investigated by dynamic light scattering DLS and photon (cross) correlation spectrometry P(C)CS. The magnetic properties are determined by static magnetization measurements M(H) in a SQUID magnetometer. The dynamic magnetic properties are measured by ac susceptibility measurements ACS, in the magnetization and the magnetic relaxation MRX, magnetic particle spectroscopy MPS and in rotating magnetic fields RMF. All these methods are grouped together in Fig. 4. The main challenge is to obtain a consistent data set of all methods applied to a nanoparticle sample.

In several projects we developed novel instruments for the fast and precise characterization of magnetic nanoparticles. Such an instrument is the Magnetic Nanoparticle Relaxation Analyzer shown in Fig. 5, which was evaluated together with Merck KGaA, Darmstadt.

Many different procedures and recipes exist for the growth of magnetic nanoparticles in solution, i.e. co-precipitation, hydrothermal synthesis, microemulsion and thermal decomposition of iron oleate. The latter has been employed successfully in the institute and the resulting nanoparticles proved to be very well reproducible [3]. These particles have been analyzed in detail by high resolution transmission electron microscopy, as depicted in Fig. 6. The inner core consists mainly of wustite FeO, while in the outer core area Fe_3O_4 (magnetite) is found. For maximum saturation magnetization the oxidation process during growth of the nanoparticles has to be carefully optimized to avoid the occurrence of such oxygen deficient phases.

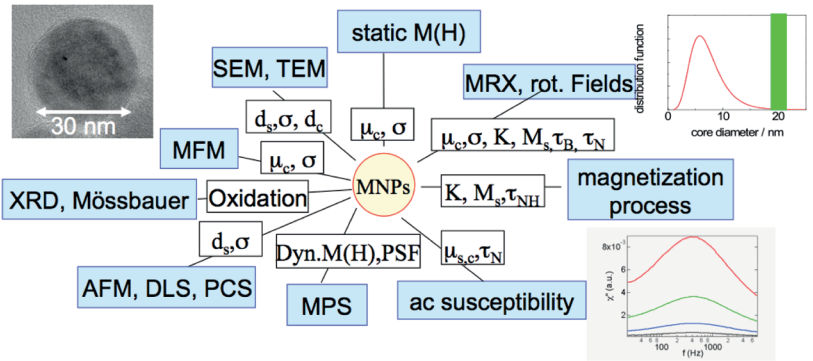

Fig. 4 Methods for the characterization of magnetic nanoparticles.

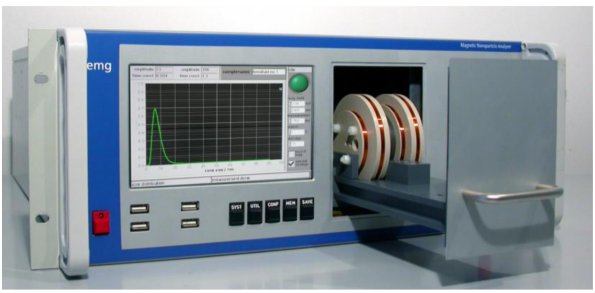

Fig. 5 MRX analyzer with coil system of high homogeneity and minimum stray field and a simple user interface with touch screen [2].

The dynamic magnetic properties are analyzed by ac susceptibility measurements (ACS) on dispersed nanoparticles and on immobilized samples from the same batch. Immobilization is easily accomplished by freeze drying. In ac susceptibility the reaction of the nanoparticles to time-dependent sinusoidal external magnetic fields is recorded and analyzed. Typical ac susceptibility measurements for multicore magnetic nanoparticles of different hydrodynamic size (increasing from FeraSpin XS to XXL) are depicted in Fig. 7. FeraSpin R particles contain a broad size distribution.

The analysis of the static M(H) SQUID magnetometer data requires a mathematical model and by assuming a bimodal distribution f(m) the magnetization M(H) can be described by [4]:

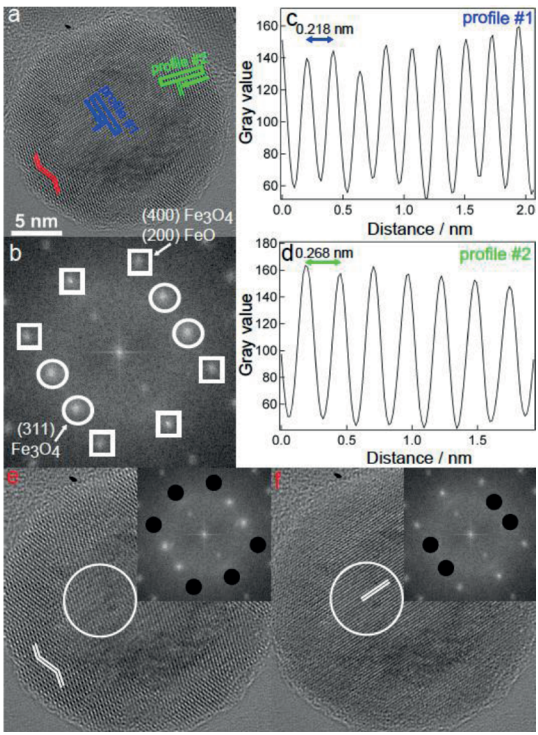

Fig. 6 Transmission electron microscopy of magnetic nanoparticles. (a)image, (b) diffraction analysis SEAD, (c,d) evaluation of lattice con-stants, (e,f) analysis of different crystalline phases in the core (FeO) and Fe_3O_4 in the outer core volume [3].The HRTEM measurements were taken in cooperation with H. Weller et al., Univ. Hamburg

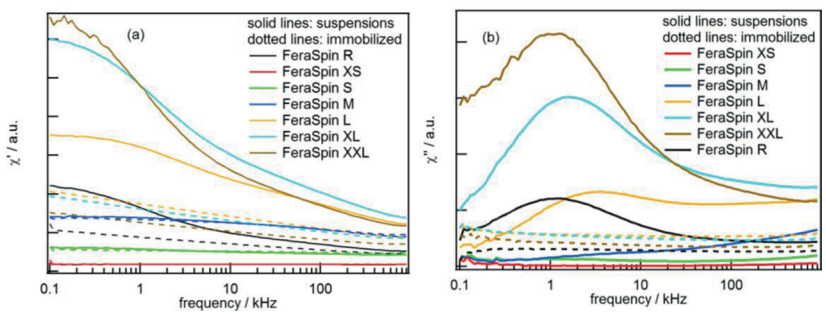

Fig. 7. AC susceptibility measurements in small signal mode (B_{ac}= 95 µT in frequency range from 100 Hz - 1 MHz).

$$M(H) = \Phi \cdot M_s \cdot \frac{1}{\overline{m}} \cdot \int m \cdot f(m) \cdot L(H,m) dm$$

By applying a SVD algorithm [5] we verified for this model the size distribution parameters according to Fig. 8.

For larger nanoparticle diameter ac susceptibility measurements become rather time consuming, since the characteristic time constants are longer for larger particles. For such particles the measurement of the magnetic relaxation MRX is more convenient. First, the particles are magnetized in an external magnetic field, then the field is switched off and the relaxation of the nanoparticle magnetization is determined by magnetic sensors. In our set-up we use either fluxgate sensors [6] or dc-SQUID sensors [7].

The recorded MRX data of the immobilized nanoparticles are shown in Fig. 9. In such measurements the contributions of larger particles can be easily detected, since the contributing frequency range can be extended to much lower frequencies than 100 Hz. The model for the measured magnetic moment m_r in the relaxation process assumes non-interacting nanoparticles. It has to take into account the time for magnetization t_{mag}, which determines the number of aligned moments in the external magnetic field H prior to the relaxation with respect to the Néel relaxation time t_{NH} in the magnetizing field H. The Langevin function L(d,H,T) determines the influence of temperature T on the alignment of nanoparticles with diameter d. The relaxation is governed by the Néel relaxation time t_N without external field. The size distribution f (lognormal distribution) has to be taken into account as well and can be obtained from these measurements by inverting the model equation [8]:

$$m_r(t,t_{mag},H) = M_s \int f(d,\mu,\sigma) \frac{\pi d^3}{6} L(d,H,T) \left\{ 1 - \exp\left[-\frac{t_{mag}}{\tau_{NH}(K,d,H,T)} \right] \right\} \exp\left[-\frac{t}{\tau_N(K,d,T)} \right] dd$$

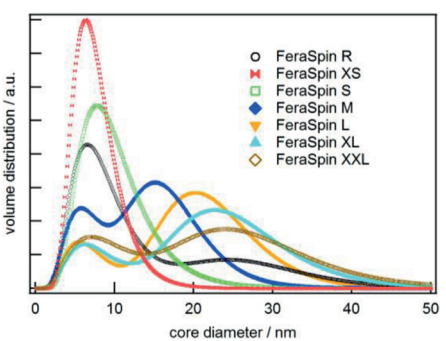

Fig. 8: Size distributions of magnetic nanoparticles with different hydrodynamic diameters.

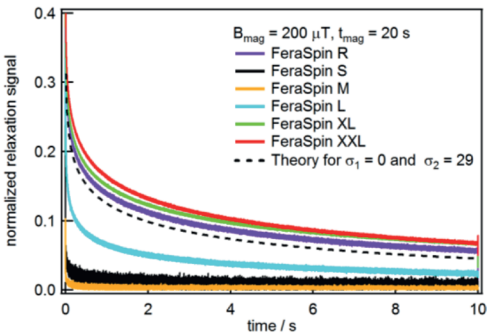

Fig. 9 MRX measurements on the same magnetic nanoparticles as in Fig. 8.

One theoretical relaxation curve is added to Fig. 9 as the dashed line for a bi-modal distribution. In samples where both Brownian and Néel relaxation take place at the same time the faster relaxation governs the experimental observed effective relaxation time as depicted in Fig. 10 with $\tau_B = \frac{3V^* \cdot \eta}{k_B \cdot T}$, $\tau_N = \tau_0 \exp\left(\frac{K \cdot V}{k_B \cdot T}\right)$ and $\tau_{eff} = \frac{\tau_B \cdot \tau_N}{\tau_B + \tau_N}$ [9].

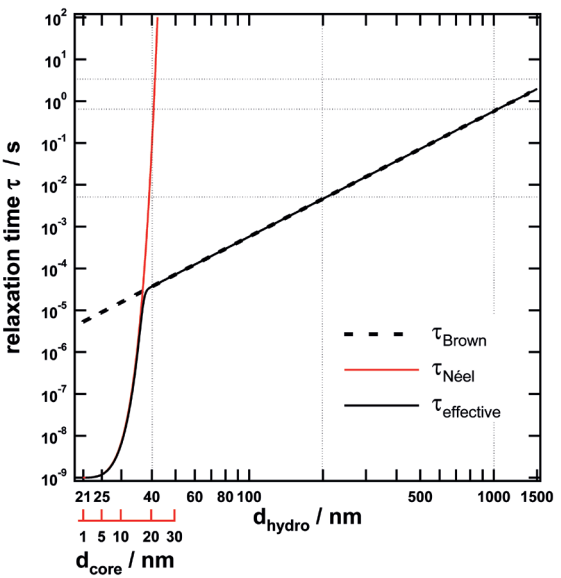

Fig. 10 Observed effective relaxation time in MRX measurements

Table 1: Possibilities to analyze and manipulate magnetic nanoparticles.

Magnetic field	**Magnetic nanoparticles**	**Used in**
Static, homogeneous	Alignment	SQUID M(H)
Switched	Relaxation	MRX Brown/Néel
Sinusoidal, low B	Alignment, Absorption	ACS ac susceptibility
2d/3d Sinusoidal, low B	Phase lag	RMF rotating fields
Sinusoidal, high B	THD	MPS Spectroscopy
Gradient	Motion	Drug delivery
Field free point	Spatial selection	Magnetic Particle Imagin
Field free point	Bound/unbound	Mobility MPI

The ACS and MRX measurements allow to determine the size distributions of magnetic nanoparticles dispersed in solution. So far water was assumed as solvent. But these methods can be extended to investigate nanoparticle interaction with the surrounding matrix characterized by the observed nanoviscosity, as depicted in Fig. 11 for $CoFe_2O_4$ nanoparticles (d_c = 15 nm) with 2.5 wt% aqueous gelatin solution together with a MRX-simulation with parameters from fits to ACS spectra [10].

In table 1 the possibilities to analyze and to manipulate magnetic nanoparticles by magnetic fields are summarized.

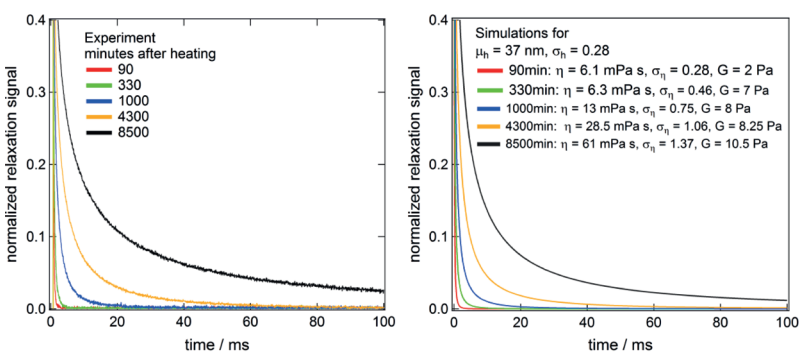

Fig. 11. Determination of the nanoviscosity of gelatine after heating and fast cooling to 23 °C from the MRX measurements during gelation.

V. Medical applications of magnetic nanoparticles

The biomedical application areas of magnetic nanoparticles are widespread. The nanoparticles can be used as markers in immunoassays and in binding-assays like in biochips based on DNA or RNA detection. They are often used as magnetic beads for separation of proteins. The demonstrated micro- and nanoviscosity measurements are used to characterize gel formation and dissolution as required for drug delivery. Functionalized nanoparticles can themselves carry drugs and be steered by external fields to the application site inside the body. The absorption of ac magnetic fields can be used to locally heat the volume around the nanoparticles in hyperthermia to drive tumor cells into apoptosis. For every mentioned application nanoparticles with special magnetic properties are required and for in-vivo applications long term stable nanoparticles without agglomeration or sedimentation are required.

A very powerful new medical imaging modality is the so called magnetic particle imaging MPI, which was invented by Gleich and Weizenecker [11] at Philips, Hamburg in 2005. Their idea was to create a point in space where the magnetic field vanishes. This can easily be accomplished by two planar coils with antiparallel orientation. Due to their combined, opposite dipole fields exactly one point in space is field free. This point can be scanned through the volume of interest by superimposed homogeneous magnetic fields from additional drive field coils in all orthogonal directions without any moving parts. If there are magnetic nanoparticles inside this volume of interest, they are exposed to a time varying magnetic field during the scanning process. Due to their nonlinear magnetization curve the nanoparticles produce different higher harmonics for certain positions of the field free point. This way the positions of the magnetic nanoparticles can be spatially decoded by the fast motion of the field free point in space and an appropriate reconstruction method. Even in the early publications already 30 images per second were demonstrated with the prospect of a simple and fast magnetic imaging modality using magnetic nanoparticles as contrast agent. One drawback are the high gradient fields occurring in this process, which might move the particles, and the high frequency fields, which might heat the tissue too much beyond the ICNIRP acceptable limits. The first MPI system built completely in the institute at TU Braunschweig is depicted in Fig. 12 [12].

The generation of higher harmonics by the magnetic nanoparticles is visualized in Fig. 13. Depending on the superimposed selection field the sinusoidal drive field has a different offset and produces the spectral fingerprint shown at the right columns.

The simulated odd harmonic spectra for one dimensional positions of the field free point symmetrically around a position at 25 units are shown in Fig. 14. For a high resolution imaging many harmonics have to be recorded, as first approxi-

Fig. 12. MPI equipment and MPI coil assembly in the EMG-institute at TU Braunschweig.

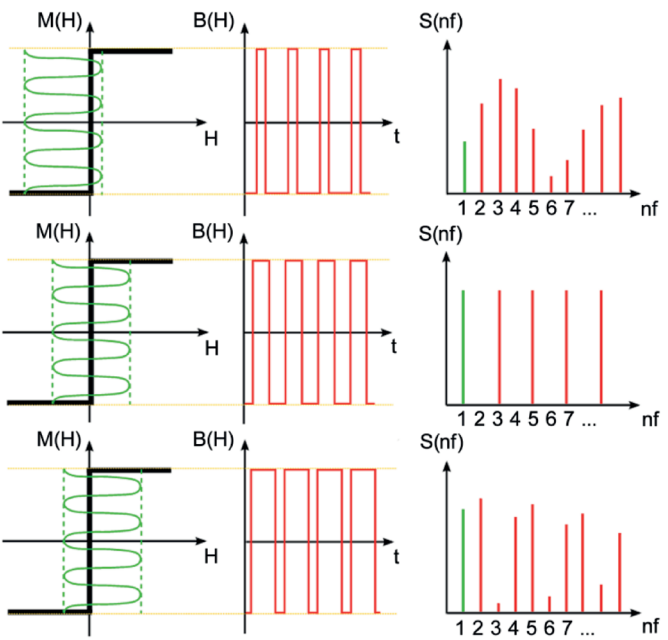

Fig. 13 Creation of higher harmonics of a sinusoidal excitation of the magnetization of magnetic nanoparticles.

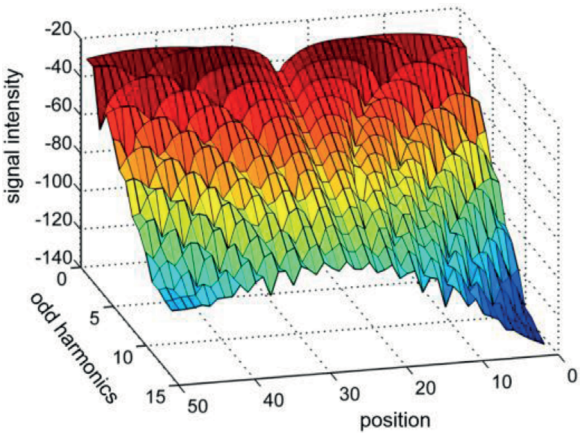

Fig. 14 Harmonic spectra for different positions of the field free point with respect to the nanoparticles.

mation the number of harmonics gives the number of pixels in one dimension. To encode the three-dimensional space, three slightly frequency shifted sinusoidal drive fields are employed, resulting in a three-dimensional Lissajous trace of the field free point to cover the whole volume of interest. The signature of the harmonic content, as recorded in the system matrix by calibration measurements before, is used by the reconstruction algorithm to image the unknown spatial nanoparticle distribution. At least three different approaches for reconstruction are pursued, as summarized in table 2. The simplest, but slowest method is to

Table 2. Different approaches for reconstruction in MPI.

Single harmonic	**Many harmonics (frequency domain)**	**X space (time domain)**
•narrow bandwidth (<< 100 Hz, resonant readout) •high sensitivity •simple reconstruction (time domain) •no reference scan required •slow (max. 1 image/s)	•large bandwidth (> 1 MHz) •Sensitivity limited by amplifier noise •complex reconstruction (frequency domain) •time-consuming reference scan •fast (> 20 images/s, real time)	•large bandwidth (> 1 MHz) •Sensitivity limited by amplifier noise •simpler reconstruction (time domain) •no reference scan •slower (better SNR for reconstruction needed)

analyze only single harmonics at a time with the advantage that a narrow band high-sensitivity receiver set-up can be employed. If many harmonics are recorded simultaneously a large bandwidth receiver is required with higher noise contribution and higher susceptibility to all kinds of external noise sources. The similar x-space reconstruction uses the time domain signals for reconstruction, but is considerably slower. So, for fast imaging the frequency domain reconstruction is preferable, despite is higher complexity [13].

VI. Conclusions and Outlook

Magnetic nanoparticles are characterized by their size dependent magnetic properties. Depending on the material they behave superparamagnetic for the size required in biomagnetic applications in the human body. For a safe and reproducible application the magnetic nanoparticles have to be characterized throughout. Quality control requires to stabilize these properties from the production to the final application in diagnosis or therapy. This is still a considerable task to achieve. For diagnosis magnetic nanoparticles can be employed as markers in Magnetic Particle Imaging MPI. This new method provides unique imaging perspectives, as quantitative marker based molecular imaging of function with an affordable imaging system. The markers are biocompatible and long-term stable. Bound and unbound particles can be distinguished by their magnetic behavior. With MPI fast imaging of 46 pics/s or 21,5 ms for full field of view are already demonstrated [14]. MPI is sensitive imaging, since as low as 100 nmol Fe are detectable in immunoassays. MPI can be combined with other imaging methods for anatomy as fluorescence superresolution microscopy by fluorescent magnetic nanoparticles, but MRI, CT and PET are also possible.

VII. Acknowledgements

The contributions of all collaborators are gratefully acknowledged, especially Frank Ludwig, who organizes the nanoparticle research in the institute for his exceptional engagement and his invaluable contributions to the field. We acknowledge financial support by SPP1681“Feldgesteuerte Partikel-Matrix-Wechselwirkungen: Erzeugung, skalenübergreifende Modellierung und Anwendung magnetischer Hybridmaterialien“, by SFB 578 „From gene to product“ and by European Commission FP7 project “Nanomag” (grant agreement no. 604448). We gratefully acknowledge support by the Braunschweig International Graduate School of Metrology B-IGSM and the DFG Research Training Group GrK1952/1 „Metrology for Complex Nanosystems.

VIII. Literature

[1] CHARBEL, T. & J. GIERALTOWSKI (2008): The Stoner-Wohlfarth model of Ferromagnetism. – Eur. J. Phys. **29**: 475–487.

[2] LUDWIG, F., E. HEIM & M. SCHILLING (2007): Characterization of superparamagnetic nanoparticles by analyzing the magnetization and relaxation dynamics using fluxgate magnetometers. – J. Appl. Phys. **101**: 113909-1-10.

[3] LAK, A. (2013): Synthesis and Characterization of Magnetic Iron Oxide Nanoparticles, Dissertation, TU Braunschweig 2013.

[4] EBERBECK, D., F. WIEKHORST, S. WAGNER & L. TRAHMS (2011): How the size distribution of magnetic nanoparticles determines their magnetic particle imaging performance. – Appl. Phys. Lett. **98**: 182502.

[5] YOSHIDA,T, K. ENPUKU, F. LUDWIG, J. DIECKHOFF, T. WAWRZIK, A. LAK & M. SCHILLING (2012): Characterization of Resovist nanoparticles for magnetic particle imaging. Magnetic Particle Imaging, Springer Proceedings. – Physics, **140**: 3–7.

[6] LUDWIG, F., S. MÄUSLELEIN, E. HEIM & M. SCHILLING (2005): Magnetorelaxometry of magnetic nanoparticles in magnetically unshielded environment utilizing a differential fluxgate arrangement. – Rev. Sci. Instrum. **76**: 106102-1–3.

[7] LUDWIG, F., E. HEIM, D. EBERBECK, K. SCHWARZ, L. TRAHMS & M. SCHILLING (2009): Comparison and calibration of fluxgate and SQUID magnetorelaxometry techniques for the characterization of magnetic core-shell nanoparticles. – IEEE Trans. Magn. **45**(10): 4857–4860.

[8] HEIM, E. (2009): Fluxgate-Magnetrelaxometrie magnetischer Nanopartikel in der Bioanalytik. – Dissertation, TU Braunschweig.

[9] WILLIAM T. COFFEY, P.J. CREGG & YURI P. KALMYKOV (1993): On the theory of Debye and Néel relaxation of single domain ferromagnetic particles. – Adv. Chem. Phys. **83**: 263.

[10] REMMER, H., J. DIECKHOFF, A. TSCHÖPE, E. ROEBEN, A.M. SCHMIDT & F. LUDWIG (2016): Dynamics of $CoFe_2O_4$ Single-Core Nanoparticles in Viscoelastic Media. – Physics Procedia, Volume **75**: 1150–1157.

[11] GLEICH, B. & J. WEIZENECKER (2005): Tomographic imaging using the nonlinear response of magnetic particles. – Nature **435**(7046): 1214–1217.

[12] MEINHARD SCHILLING, M., F. LUDWIG, C. KUHLMANN & T. WAWRZIK (2013): Magnetic Particle Imaging-Scanner with 10 kHz drive-field frequency. – Biomed Tech (Berl). **58**(6): 557–63.

[13] VIERECK,T. (2016): Magnetic Particle Imaging – Dissertation, TU Braunschweig.

[14] WEIZENECKER, J., B. GLEICH, J. RAHMER, H. DAHNKE & J. BORGERT, (2009): Three-dimensional real-time in vivo magnetic particle imaging. – Phys. Med. Biol. **54**: L1–L10.